# Photometric Distance to the RR Lyrae Star SW Andromedae Using Period-Luminosity-Metallicity Relationships

**Talon Dow**
**Jakob Bergstedt**
**Emily Payne**
**Tyce Olaveson**
**Hayley Kerkman**
**Lesilie Greer**
**Stephen McNeil**

*Brigham Young University-Idaho, Department of Physics, Rexburg, ID 83460; address correspondence to mcneils@byui.edu*

*Received July 15, 2022; revised March 24, 27, 2023; accepted March 29, 2023*

**Abstract** Cáceres and Catelans' period-luminosity-metallicity equations give us a way to measure the photometric distance to RR Lyrae stars using absolute magnitude equations that rely on the specific photometric filter (V, i, and z), the period, and the metallicity. Over a period of two weeks, 76 images of the RR Lyr Star SW Andromedae were taken in the B, V, i, and z bands. Using Source Extractor Kron (SEK) photometry method, the apparent magnitudes were plotted and converted into periods and amplitudes. Together with previously measured values for the metallicity and interstellar extinction, we calculated a photometric distance to SW Andromedae of 516 ± 14 parsecs to 527 ± 14 depending on the chosen metallicity. This distance is comparable to the parallax distance obtained from GAIA EDR3 data of 510 ± 7 parsecs.

## 1. Introduction

In the optical passbands RR Lyrae stars are connected to the metallicity by a luminosity-metallicity relationship (Clementini *et al.* 2003; Catelan *et al.* 2004; Marconi *et al.* 2015; Muraveva *et al.* 2018; Garofalo *et al.* 2022), and in the near and mid-infrared passbands by a period-luminosity-metallicity (PLZ) relationship (Catelan *et al.* 2004; Marconi *et al.* 2015; Muraveva *et al.* 2015; Neeley *et al.* 2019). Catelan *et al.* (2004) derived the following relation for the V-band:

$$M_V = 2.288 + 0.822\,\mathrm{LogZ} + 0.108\,(\mathrm{LogZ})^2 \quad (1)$$

Cáceres and Catelan (2008) published the following PLZ equations in the i and the z bands:

$$M_i = 0.908 - 1.035\,\mathrm{LogP} + 0.220\,\mathrm{LogZ} \quad (2)$$
$$M_z = 0.839 - 1.295\,\mathrm{LogP} + 0.211\,\mathrm{LogZ}, \quad (3)$$

with the LogZ in these equations being related to the metallicity by:

$$\mathrm{LogZ} = [M/H] - 1.765 \quad (4)$$

$$[M/H] = [Fe/H] + \log(0.638 \times 100.3 + 0.362) \quad (5)$$

This paper examines the light curves for the RR Lyr star SW Andromedae using Bessel B and V filters, and SDSS/PanSTARRS i and z filters. The period and apparent magnitude will then be determined, and a distance calculated using the absolute magnitudes determined by the Cáceres and Catelan equations. This photometric distance will then be compared to the parallax distance found by GAIA EDR3 (Gaia Collaboration *et al.* 2021).

SW And has been studied by both recent surveys, including multicolor photometry (Barcza and Benkő 2014), and in the older uvbyβ photometry system (McNamara and Feltz 1977). However, there have been no papers that have used observed photometric data to determine the photometric distance to SW And using Cáceres and Catelans' equations. The general properties of SW And were obtained from SIMBAD (Wenger *et al.* 2000) and the AAVSO International Variable Star Index (VSX; Watson *et al.* 2014). This basic information is listed in Table 1.

There are a variety of published values for the metallicity of SW And, with the metallicity values ranging from –0.06 to –0.21 for metallicities based on spectra (see Table 2 for a list). For this paper, the two values of [Fe/H] = –0.06 and –0.21 will be used to see how this range affects the distance measurements.

## 2. Observations

Observations were made using the remote telescopes operated by the Las Cumbres Observatory (Brown *et al.* 2013). The telescopes were 0.4-meter with SBIG 6303 cameras, located at the Canary Islands (Spain), Fort Davis (Texas, USA), and Haleakala (Hawaii, USA). We collected images through B, V, i, and z filters. For each of these passbands, a cadence was created starting on 28 September 2020 and ending on 18 October 2020. The B band had an exposure time of 22 seconds, the V band 16, the i band 12, and the z band 38. A total of 76 images were obtained from each filter after poor quality images were thrown out. An image taken in the V filter during this observing run can be seen in Figure 1 (SW And is in the center of the image).

All images were processed using the data pipeline created by Our Solar Siblings (Fitzgerald 2018). The pipeline cleaned up all the raw images through image reduction and calibration, including noise reduction, cosmic ray removal, and flat fielding effects. This pipeline also created photometry files using both aperture photometry and point spread function photometry. For each of the four filters, six different photometry algorithms were used. These methods were Dominion Astrophysical Observatory

Table 1. General information of SW And.

| | |
|---|---|
| Right Ascension (J2000) | $00^h\ 23^m\ 43.0896^s$ |
| Declination (J2000) | +29° 24' 03.6265" |
| Period | 0.44226 day |
| Parallax (GAIA EDR3) | 1.9615 ± 0:0284 mas |
| Radial Velocity | –20.80 km/s |
| Spectral Type | A7III-F8III |

Table 2. Calculated metallicity [Fe/H] based on spectra.

| *Value* | *Measurement* |
|---|---|
| –0.06 | Clementini et al. (1995) |
| –0.07 | Liu et al. (2013) |
| –0.20 | Lambert et al. (1996) |
| –0.21 | Takeda (2022) |

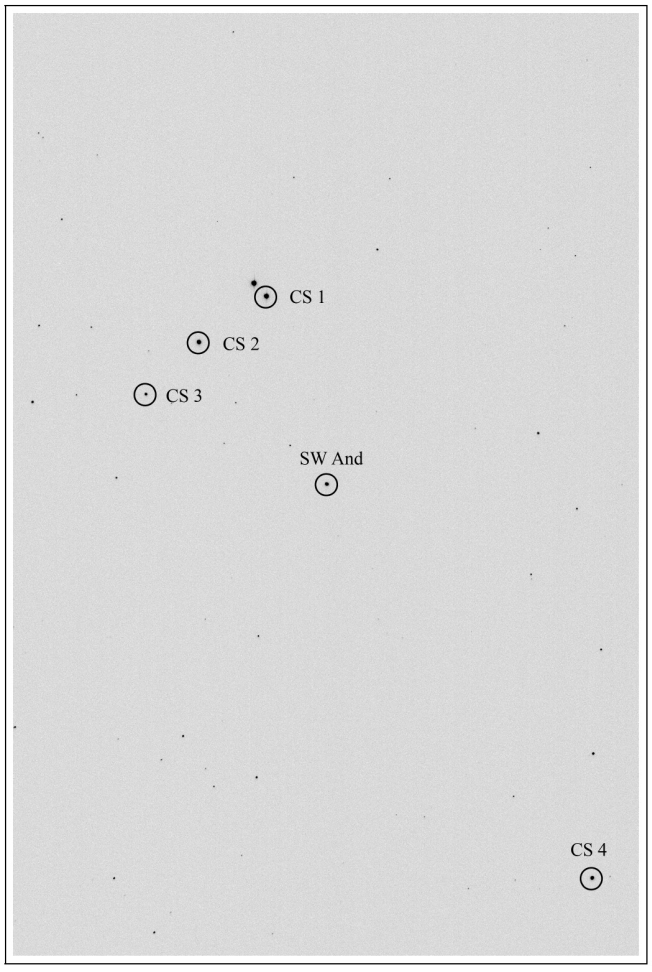


Figure 1. LCO Image of SW And using a Bessel V filter. Comparison stars (CS) used are indicated. The image is 29 × 19 arcminutes in size with north up and east to the left.

Photometry (DAOPHOT; Stetson 1987), DoPHOT (Schechter *et al.* 1993), Point Spread Function with Source Extractor (PSFEx; Bertin 2011), Source Extractor Aperture (SEX) and Source Extractor Kron (SEK) (Bertin and Arnouts 1996), and Aperture Photometry Tool (APT; Laher *et al.* 2012a, 2012b). The cleanest data set was found using the photometry method of Source Extractor using a Kron radius (SEK), so this method is the one used in this study for all the photometry.

## 3. Methods

After the data were processed using the OSS pipeline, a PYTHON program called ASTROSOURCE (Fitzgerald *et al.* 2020) was used to determine the period and amplitude and generate light curves for each of the filters. The ASTROSOURCE software analyzes the star field in each image and identifies suitable comparison stars by choosing those stars with the least variance. The star catalogs used depended on which catalog covered that part of the sky and which one was more sensitive to that particular magnitude and color. For the B, V, and i bands, the APASS star catalog (Levine *et al.* 2018) was used, and for the z band the SDSS star catalog (Alam *et al.* 2015) was used. See Table 3 for the calibrated apparent magnitudes for the comparison stars.

To account for the interstellar dust that affects the stellar magnitudes, observations in the B filter were made to help adjust the measurements in other filters by using the interstellar reddening E(B–V). The value for E(B–V) was chosen to be 0.039 based on the value found on the Galactic Dust Reddening and Extinction web page found at the NASA/IPAC Infrared Science Archive (Schlegel *et al.* 1998; Schlafly and Finkbeiner 2011). The extinction for each filter was then calculated using the extinction law equations as found in Cardelli *et al.* (1989). The calibrated apparent mid-point magnitudes, corrected for interstellar extinction, are shown in Table 4. The errors quoted in the table are from both the estimated noise from individual measurements as well as the measured standard deviation of the calibration fit.

## 4. Results

As can be seen from Figures 2, 3, 4, and 5, our light curves obtained are reminiscent of RRab type stars with a steep rise and gradual fall.

The Cáceres and Catelan equations mentioned previously allow us to take our derived periods and metallicity and convert them into an absolute magnitude. The periods were estimated using three different methods, Phase Dispersion Minimization (PDM; Stellingwerf 1978), String Method (SM; Dworetsky 1983), and the Lomb–Scargle periodogram (VanderPlas 2018). Since all three methods gave similar results, we averaged all three methods through all four filters and came up with a period of 0.44214 ± 0.00018 day. This aligns closely with the published period value on the AAVSO website (VSX) of 0.442262 day, giving us some confidence in our method of period analysis.

The measured periods and light curve amplitudes can be seen in Table 5, a Lomb-Scargle periodogram in Figure 6, and a PDM likelihood plot in Figure 7. The results were also

Table 3. Calibrated apparent magnitudes for comparison stars.

| *Star* | *R.A. (deg)* | *Dec. (deg)* | *Filters* | *B Magnitude* | *V Magnitude* | *i magnitude* | *z Magnitude* |
|---|---|---|---|---|---|---|---|
| CS 1 | 5.964772 | 29.49598 | B,V | 8.720 ± 0.090 | 8.328 ± 0.046 | — | — |
| CS 2 | 6.004061 | 29.47281 | B,V,i,z | 9.151 ± 0.085 | 8.739 ± 0.046 | 8.645 ± 0.019 | 8.905 ± 0.019 |
| CS 3 | 6.034822 | 29.44641 | i,z | — | — | 10.041 ± 0.020 | 10.069 ± 0.028 |
| CS 4 | 5.775393 | 29.20150 | z | — | — | — | 9.032 ± 0.020 |

Table 4. Calibrated apparent mid-point magnitudes (corrected for extinction) for SW And.

| *Filter* | *m* | *Error* |
|---|---|---|
| $B_0$ | 9.602 | 0.088 |
| $V_0$ | 9.400 | 0.046 |
| $i_0$ | 9.493 | 0.0094 |
| $z_0$ | 9.788 | 0.019 |

Table 5. Period and light curve amplitudes for B, V, i, and z filters.

| *Filter* | *DM Period* | *PDM Period* | *LS Period* | *Amplitude* |
|---|---|---|---|---|
| B | 0.44200 | 0.44200 | 0.44220 | 1.386 |
| V | 0.44240 | 0.44190 | 0.44240 | 1.014 |
| i | 0.44200 | 0.44281 | 0.44240 | 0.653 |
| z | 0.44200 | 0.44200 | 0.44219 | 0.580 |

Table 6. Absolute magnitudes (M) and extinction (A) for SW And.

| *Filter* | *M* | *A* |
|---|---|---|
| V | 1.069 ± 0.051 | 0.121 |
| i | 0.887 ± 0.022 | 0.0826 |
| z | 0.926 ± 0.021 | 0.0595 |

Table 7. Photometric distance to SW And.

| *Filter* | *Distance [Fe/H] = –0.06* | *Distance [Fe/H] = –0.21* |
|---|---|---|
| V | 447 ± 32 | 464 ± 33 |
| i | 518 ± 19 | 526 ± 19 |
| z | 584 ± 21 | 592 ± 21 |
| Viz | 516 ± 14 | 527 ± 14 |

compared to TESS data (Ricker *et al.* 2015), obtained through the software Peranso (Paunzen and Vanmunster 2016), which can be seen in Figures 8 and 9. The TESS data spanned the time from 8 October 2019 to 31 October 2019. As can be seen from the almost perfect observed light curve from the TESS data, their period has a much lower experimental error. Using Peranso and the ANOVA method (Schwarzenberg-Czerny 1996) for period analysis, a TESS period of 0.442263 ± 0.000020 day is found. This is the period which will be used in all our calculations, since it has the smallest measurement error.

## 5. Discussion and analysis

The purpose of this research was to determine if the photometric distance as calculated through period-luminosity-metallicity equations for RR Lyr stars from Catelan *et al.* (2004) and Cáceres and Catelan (2008) agrees with GAIA EDR3 parallax distances. In order to calculate the photometric distance to SW And we used the standard distance equation:

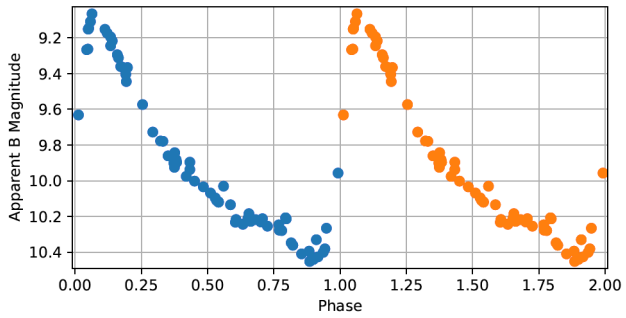


Figure 2. B filter phased light curve for SW And.

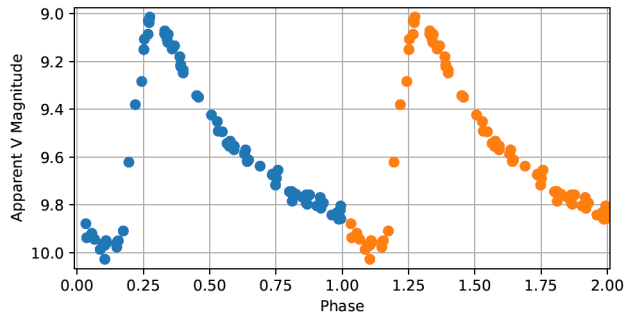


Figure 3. V filter phased light curve for SW And.

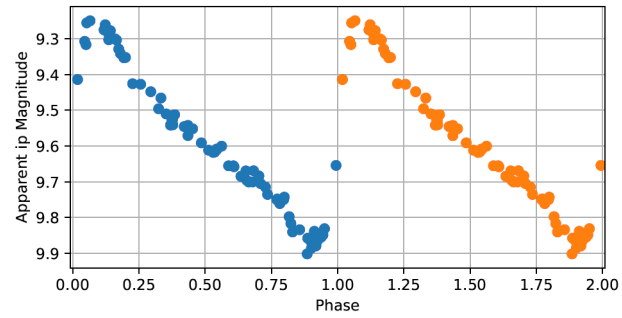


Figure 4. i filter phased light curve for SW And.

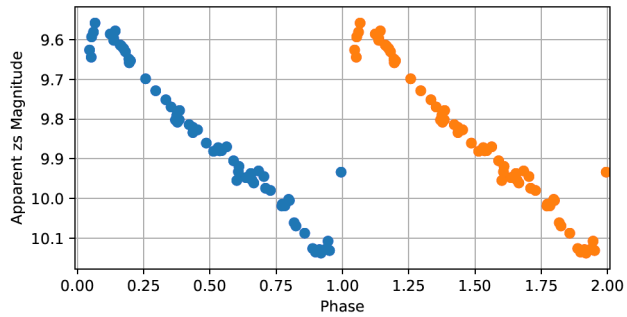


Figure 5. z filter phased light curve for SW And.

$$d = 10^{(m - M - A + 5)/5}, \quad (6)$$

where m is our measured apparent mid-magnitude in each filter, M is the absolute magnitude as calculated using the Cáceres and Catelan equations (using the period and metallicity), and A is the extinction at a specific wavelength and is based on an interstellar reddening of E(B–V) = 0.039 as discussed previously in section 3. This information is found in Table 6.

Using the values given in Table 6, an average photometric distance to SW And is calculated through all three filters of 516 ± 14 parsecs for [Fe/H] = –0.06 and 527 ± 14 for [Fe/H] = –0.21. These averages compare relatively well to the parallax distance obtained from GAIA EDR3 data of 510 ± 7 parsecs and roughly overlap the GAIA data within the margin of error. However, as can be seen in Table 7, individual filter distances can either be well below or well above the GAIA distance. Although the i filter distance compares relatively well with GAIA, the other two filters are clearly a couple of standard deviations away from this average. A possible reason for the V filter being off at a value of [Fe/H] = –0.06 is that this is really beyond the metal-rich end for the data range cited in Catelan *et al.* (2004). However, [Fe/H] = –0.21 is not, but suffers from the same underestimation. As a comparison, at least in the V filter, the data was also used in the PZ relationship developed by Garofalo *et al.* (2022) for RR Lyr field stars, which gave a distance of 455 ± 4 to 465 ± 3 for the range of Fe/H of –0.06 to –0.21. These calculated distances are almost the same, albeit with a smaller error, as the distances using Cáceres and Catelans' PZ equation.

## 6. Conclusion

The goal of this project was to test the validity of Cáceres and Catelans' period-luminosity-metallicity equations for RR Lyr field stars using SW And. The validity is tested by comparing our calculated photometric distance, based on the magnitudes derived using the PLZ equations, to the calculated parallax distance from GAIA EDR3 data. Using the data we acquired and previously measured interstellar reddening and metallicity values, the average distance (through V, i, and z filters) was calculated to be 516 ± 14 parsecs or 527 ± 14 parsecs, depending on the metallicity used. Both of these averages are within one standard deviation of the current parallax distance as measured by GAIA, 510 ± 7 parsecs. This seems to support the validity of Cáceres and Catelans' equations in this limited study of just one RR Lyr field star. The i filter distance matched GAIA the best, and may suggest a better correlation to distance, but to confirm that would require considerably more i filter data using other RR Lyr stars. Since the distance is dependent on metallicity and interstellar reddening, having definitive values for both [Fe/H] and E(B–V) would help with reducing the error on the photometric distance. The discrepancy in distance for the various filters will need to be looked at further in any future studies, since taking a straight average of V, i, and z may have complications tied to how well the PLZ equations actually fit the data used to develop those equations in the different filters.

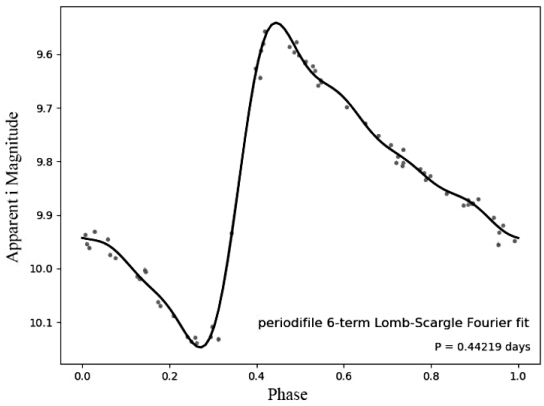


Figure 6. Lomb-Scargle light curve fit using the i filter.

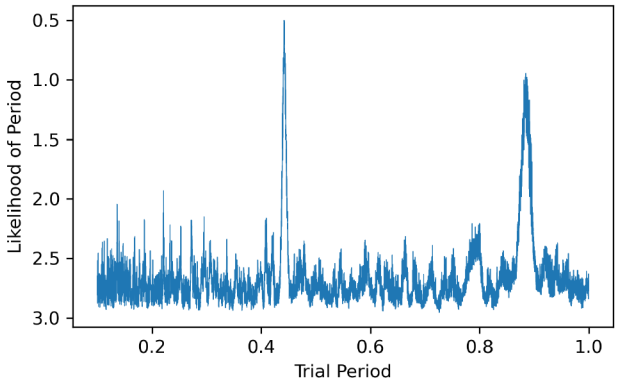


Figure 7. Likelihood plot for the period of SW And.

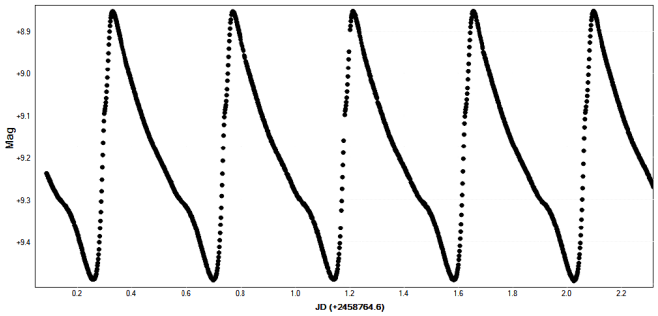


Figure 8. TESS light curve for SW And over several periods.

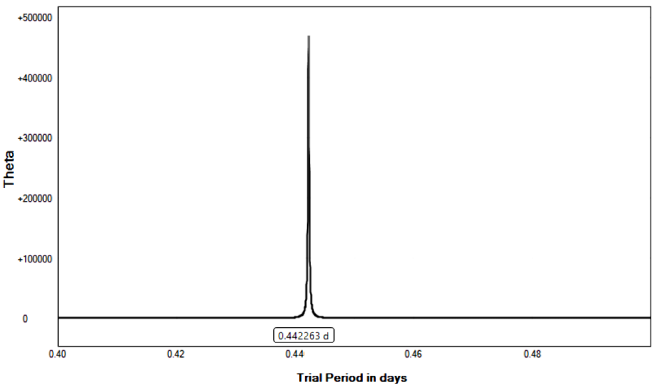


Figure 9. Peranso period analysis of the TESS light curve using the ANOVA method.

**7. Acknowledgements**

The authors would like to acknowledge Michael Fitzgerald and Our Solar Siblings for providing this research opportunity and providing our group with a plethora of knowledge concerning variable stars and RR Lyr stars.

This research made use of Peranso (www.peranso.com), a light curve and period analysis software. This research has also made use of the Aladin Sky Atlas, SIMBAD, and VizieR developed at CDS, Strasbourg Observatory, France. We acknowledge with thanks the variable star observations from the AAVSO International Database contributed by observers worldwide and used in this research.

**References**

Alam, S., *et al.* 2015, *Astrophys. J., Suppl. Ser.*, **219**, 12 (DOI: 10.1088/0067-0049/219/1/12).

Barcza, S., and Benkő, J. M. 2014, *Mon. Not. Roy. Astron. Soc.*, **442**, 1863 (DOI: 10.1093/mnras/stu978).

Bertin, E. 2011, in *Astronomical Data Analysis Software and Systems XX*, eds. I. N. Evans, D. J. Mink, A. H. rots, ASP Conf. Proc. 442, Astronomical Society of the Pacific, San Francisco, 435.

Bertin, E., and Arnouts, S. 1996, *Astron. Astrophys., Suppl. Ser.*, **117**, 393 (DOI: 10.1051/aas:1996164).

Brown, T. M., *et al.* 2013, *Publ, Astron. Soc. Pacific*, **125**, 1031 (DOI: 10.1086/673168).

Cáceres, C., and Catelan, M. 2008, *Astrophys. J., Suppl. Ser.,* **179**, 242 (DOI: 10.1086/591231).

Cardelli, J. A., Clayton, G. C., and Mathis, J. S. 1989, *Astrophys. J.*, **345**, 245 (DOI: 10.1086/167900).

Catelan, M., Pritzl, B. J., and Smith, H. A. 2004, *Astrophys. J., Suppl. Ser.*, **154**, 633 (DOI: 10.1086/422916).

Clementini, G., Carretta, E., Gratton, R., Merighi, R., Mould, J. R., and McCarthy, J. K. 1995, *Astron. J.*, **110**, 2319 (DOI: 10.1086/117692).

Clementini, G., Gratton, R., Bragaglia, A., Carretta, E., Di Fabrizio, L., and Maio, M. 2003, *Astron. J.*, **125**, 1309 (DOI: 10.1086/367773).

Dworetsky, M. 1983, *Mon. Not. Roy. Astron. Soc.*, **203**, 917.

Fitzgerald, M. T., Cutts, R., Salimpour, S., and Slater, S. 2018, *Robotic Telesc. Student Res. Education Proc.*, **1**, 1.

Fitzgerald, M., Gomez, E., Salimpour, S., and Wibowo, R. 2020, *J. Open Source Software*, in review.

Gaia Collaboration, Brown, A. G. A., *et al.* 2021, *Astron. Astrophys.*, **649A**, 1 (DOI: 10.1051/0004-6361/202039657).

Garofalo, A., Delgado, H. E., Sarro, L. M., Clementini, G., Muraveva, T., Marconi, M., and Ripepi, V. 2022, *Mon. Not. Roy. Astron. Soc.*, **513**, 788 (DOI: 10.1093/mnras/stac735).

Laher, R. R., Gorjian, V., Rebull, L. M., Masci, F. J., Fowler, J. W., Helou, G., Kulkarni, S. R., and Law, N. M. 2012a, *Publ. Astron. Soc. Pacific*, **124**, 737.

Laher, R. R., *et al.* 2012b, *Publ. Astron. Soc. Pacific*, **124**, 764.

Lambert, D. L., Heath, J. E., Lemke, M., and Drake, J. 1996, *Astrophys. J., Suppl. Ser.*, **103**, 183 (DOI: 10.1086/192274).

Levine, S., Henden, A., Terrell, D., Welch, D., and Kloppenborg, B. 2018, in *AAS/Division for Planetary Sciences Meeting Abstracts, Vol. 50*, AAS/Division for Planetary Sciences Meeting Abstracts #50, 315.03.

Liu, S., Zhao, G., Chen, Y.-Q., Takeda, Y., and Honda, S. 2013, *Res. Astron. Astrophys.*, **13**, 1307 (DOI: 10.1088/1674-4527/13/11/003).

Marconi, M., *et al.* 2015, *Astrophys. J.*, **808**, 50 (DOI: 10.1088/0004-637X/808/1/50).

McNamara, D. H., and Feltz, K. A., Jr. 1977, *Publ. Astron. Soc. Pacific*, **89**, 699 (DOI: 10.1086/130212).

Muraveva, T., Delgado, H. E., Clementini, G., Sarro, L. M., and Garofalo, A. 2018, *Mon. Not. Roy. Astron. Soc.*, **481**, 1195 (DOI: 10.1093/mnras/sty2241).

Muraveva, T., *et al.* 2015, *Astrophys. J.*, **807**, 127 (DOI: 10.1088/0004-637X/807/2/127).

Neeley, J. R., *et al.* 2019, *Mon. Not. Roy. Astron. Soc.*, **490**, 4254 (DOI: 10.1093/mnras/stz2814).

Paunzen, E., and Vanmunster, T. 2016, *Astron. Nachr.*, **337**, 239 (DOI: 10.1002/asna.201512254).

Ricker, G. R., *et al.* 2015, *J. Astron. Telesc. Instrum. Syst.*, **1**, 014003 (DOI: 10.1117/1.JATIS.1.1.014003).

Schechter, P. L., Mateo, M., and Saha, A. 1993, *Publ. Astron. Soc. Pacific*, **105**, 1342.

Schlafly, E. F., and Finkbeiner, D. P. 2011, *Astrophys. J.*, **737**, 103 (DOI: 10.1088/0004-637X/737/2/103).

Schlegel, D. J., Finkbeiner, D. P., and Davis, M. 1998, *Astrophys. J.*, **500**, 525 (DOI: 10.1086/305772).

Schwarzenberg-Czerny, A. 1996, *Astrophys. J., Lett.*, **460**, L107 (DOI: 10.1086/309985).

Stellingwerf, R. F. 1978, *Astrophys. J.*, **224**, 953 (DOI: 10.1086/156444).

Stetson, P. B. 1987, *Publ. Astron. Soc. Pacific*, **99**, 191.

Takeda, Y. 2022, *Mon. Not. Roy. Astron. Soc.*, **514**, 2450 (DOI: 10.1093/mnras/stac1431).

VanderPlas, J. T. 2018, *Astrophys. J., Suppl. Ser.*, **236**, 16 (DOI: 10.3847/1538-4365/aab766).

Watson, C., Henden, A. A., and Price, C. A. 2014, AAVSO International Variable Star Index VSX (Watson+, 2006–2014; https://www.aavso.org/vsx).

Wenger, M., *et al.* 2000, *Astron. Astrophys., Suppl. Ser.*, **143**, 9 (DOI: 10.1051/aas:2000332).